

Total Proton-Proton Cross Section at $s^{1/2} = 30$ TeV

R. M. Baltrusaitis, G. L. Cassiday, J. W. Elbert, P. R. Gerhardy,
S. Ko, E. C. Loh, Y. Mizumoto, P. Sokolsky, and D. Steck
University of Utah, Salt Lake City, Utah 84112

(Received 16 January 1984)

We have measured the proton-air inelastic cross section at $s^{1/2} = 30$ TeV by observing the distribution of extensive-air-shower maxima as a function of atmospheric depth. This distribution has an exponential tail whose slope is $\lambda = 72 \pm 9$ g cm $^{-2}$ which implies that $\sigma_{p\text{-air}}^{\text{inel}} = 530 \pm 66$ mb. Using Glauber theory and assuming that the elastic-scattering slope parameter b is proportional to σ_{pp}^{tot} , we infer a value of $\sigma_{pp}^{\text{tot}} = 120 \pm 15$ mb which lies between a log s and a log 2s extrapolation of the total pp cross section as measured at lower energies.

PACS numbers: 13.85.Lg, 13.85.Tp, 94.40.Pa, 94.40.Rc

The University of Utah "fly's eye" detector $^{1-4}$ records the passage of extensive air showers (EAS) through the atmosphere via the atmospheric fluorescence technique. The detector consists of 880 photomultipliers arranged in clusters of 12 or 14 and mounted in the focal plane of one of 67 1.6-m 2 mirrors. Almost the entire 2π sr night sky is imaged. By recording the arrival times and pulse integrals of each photomultiplier viewing a passing EAS, its overall longitudinal development profile can be reconstructed. The technique used to infer the proton-air inelastic cross section, $\sigma_{p\text{-air}}^{\text{inel}}$, is based on the notion that cosmic-ray protons interact in the atmosphere at rates which decrease exponentially with increasing slant depth. Thus, a direct observation of the distribution of first interactions would yield the nucleon-air interaction length λ_n . The point of first interaction cannot be observed. However, the depth of maximum of the resultant extensive air shower can be observed and its distribution also has an exponential tail 5 whose slope is $\lambda = 1.6\lambda_n$. (The value of the proportionality con-

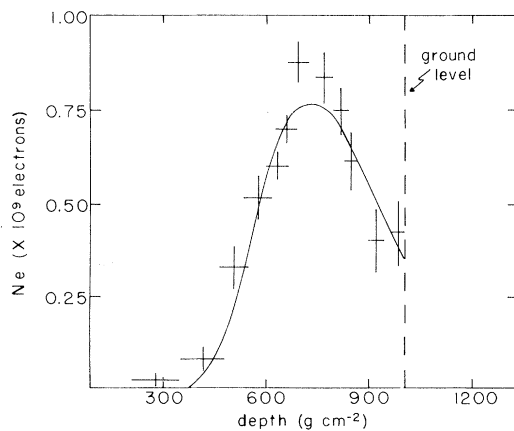


FIG. 1. An extensive air shower that survives all data cuts. The curve is a Gaisser-Hillas (Ref. 4) shower-development function; shower parameters $E = 1.3$ EeV and $X_{\text{max}} = 727 \pm 33$ g cm $^{-2}$ give the best fit.

stant is model dependent with an uncertainty of 10%. Moreover, the proportionality is strictly true only if λ is greater than the radiation length in air (~ 37 g cm $^{-2}$). 6 Thus, $\sigma_{p\text{-air}}^{\text{inel}}$ can be inferred from a measurement of the depth of maximum absorption length λ .

Shown in Fig. 1 is the longitudinal development profile of a well measured shower. A Gaisser-Hillas 1,2 shower development function was fitted to the data points, $N_e(x)$, and its depth of maximum found to be $X_{\text{max}} = 727 \pm 33$ g cm $^{-2}$. The error in X_{max} arises almost entirely from geometrical reconstruction errors in shower zenith angle, θ_z . Moreover, since atmospheric density varies exponentially with depth, symmetric errors in θ_z lead to an asymmetric bias of events towards large depths of maxima.

Additional bias toward large depths of maxima could originate from the highest-energy cosmic-ray events in the data sample. Shown in Fig. 2 is the

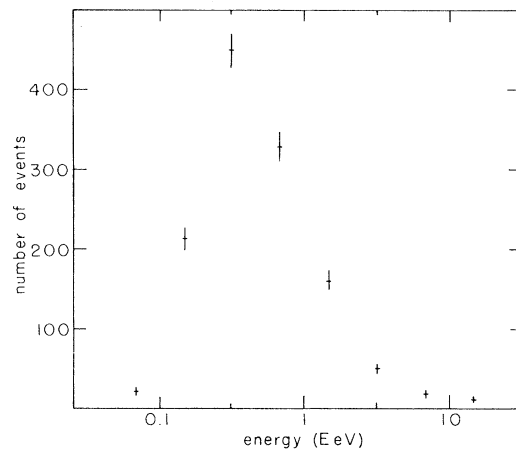


FIG. 2. Uncut energy distribution. To remove possible energy-dependent biases in resultant depth of maximum distributions only events within the interval 0.1–2.0 EeV have been accepted. \bar{E} for this sample is 0.5 EeV.

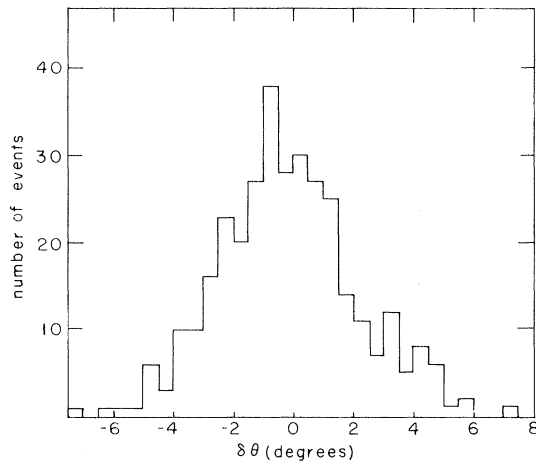


FIG. 3. Distribution of differences between known and fitted zenith angles for "upward-going" showers of known geometry generated by a high intensity light flasher. The width of the distribution is $\sigma = 1.7^\circ$. The distribution agrees well with one calculated from a distribution of estimated track fitting errors.

measured energy distribution for all accepted events. The rising edge of the distribution is due to limited acceptance at low energies while the falling edge reflects the power-law nature of the primary spectrum. Since depths of maxima vary only logarithmically with energy (about 60 g cm^{-2} per decade) rejecting all events outside the interval $0.1\text{--}2.0 \text{ EeV}$ ($1 \text{ EeV} = 10^{18} \text{ eV}$) eliminates any energy-dependent asymmetrical bias toward large depths of maxima.

An assessment of possible geometrical reconstruction bias has been carried out by analyzing a sample of tracks of known geometry generated by a mobile light flasher unit. A pulse of light generated by this unit has been fired over the "fly's eye" detector from a variety of positions and in a variety of directions. The scattered light from this propagating light pulse simulates the light emission process of a real event and its trajectory can thus be reconstructed in the same way as that of a real event. Shown in Fig. 3 is the distribution of differences between the known and fitted zenith angles for all such trajectories. The σ of the distribution (1.7°) agrees well with the most probable error of 1.75° obtained from the data fits exclusively. In fact, the entire distribution is identical to a calculated one that is a sum of Gaussians whose σ 's are distributed according to the distribution of estimated angular errors obtained from track reconstruction data fits. This agreement implies that geometrical reconstruction errors are well understood.

We show in Fig. 4 the resultant distribution of

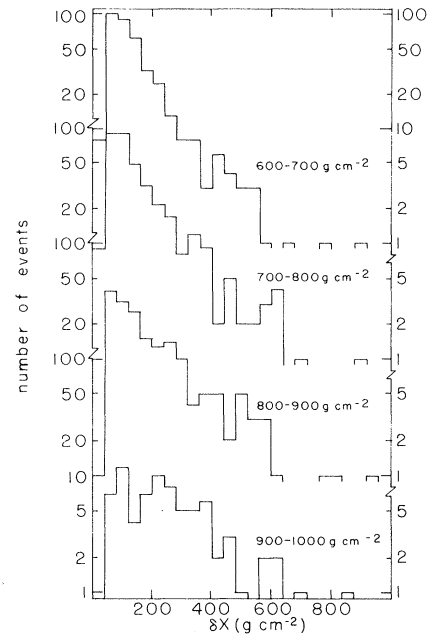


FIG. 4. Distribution of fitting errors for all real events with energies in the interval $0.1\text{--}2.0 \text{ EeV}$. Data have been grouped into four 100 g cm^{-2} depth intervals with X_{max} ranging from 600 to 1000 g cm^{-2} . Each histogram spans roughly two decades. The lower portion of each histogram can be read from the right scale while the upper portion can be read from the left scale. The mode, mean, and width of each distribution are shown in Table I along with the results for an unplotted distribution of data in the $1000\text{--}1100 \text{ g cm}^{-2}$ interval.

fitting errors, δx , in depth of shower maximum for each real event. The data have been grouped into four 100 g cm^{-2} intervals with X_{max} ranging from 600 g cm^{-2} to 1000 g cm^{-2} . Since events at large depth of maximum are preferentially selected at large zenith angles we expect the errors δx to increase with X_{max} . This effect can be seen in Table I which lists the mode, average, and width of each distribution in Fig. 4 (and also for an unplotted distribution in the depth interval $1000\text{--}1100 \text{ g cm}^{-2}$). The large x bias can be eliminated by excluding events which have errors in X_{max} greater than a cut value δx_c . As an example, the results of applying a 125 g cm^{-2} data cut are shown in Table I where it can be seen that the mode, average, and width of the cut distribution have become independent of x .

Shown in Fig. 5 is the resultant X_{max} distribution which satisfies the $\delta x < 125 \text{ g cm}^{-2}$ cut. Its mean δx is $\sim 70 \text{ g cm}^{-2}$. One might expect that the tail of this distribution could be somewhat flattened due to the 70 g cm^{-2} resolution. Such is not the case. If one folds a Gaussian resolution function (or a sum of Gaussians, which is a reasonable ap-

TABLE I. Most probable value (mode), average, and width of the distribution of depth of maximum measurement errors for five different 100 g cm^{-2} depth intervals. The bias of the error distribution towards larger depths is obvious in the uncut data sample. In the cut data sample bias has been essentially eliminated. All data values are in grams per square centimeter.

Depth interval	δx Mode	Uncut data		125 g cm^{-2} cut		
		δx Average	$\sigma(\delta x)$ Width	δx Mode	δx Average	$\sigma(\delta x)$ Width
600–700	75	149	118	75	86	24
700–800	75	160	130	75	80	25
800–900	70	203	161	70	80	20
900–1000	95	261	175	95	87	20
1000–1100	200	341	229

proximation of our “cut” error distributions) into an exponential distribution, the slope of the distribution is preserved. The only effect of finite resolution is to broaden the portion of the curve near the peak. At distances on the order of $(\delta x)^2/\lambda$ away from the peak, the exponential slope of the experimental distribution approaches that of the true one. Since both λ and δx are on the order of $\sim 70 \text{ g cm}^{-2}$, the true exponential character of the plot should appear at depths $X_{\text{max}} > 800 \text{ g cm}^{-2}$. A best fit to the data for $X_{\text{max}} > 830 \text{ g cm}^{-2}$ yields $\lambda = 73 \pm 9 \text{ g cm}^{-2}$. Shown in Table II are the results of fits to the X_{max} distributions generated by applying progressively more restrictive data cuts. In each case λ was obtained by fitting the X_{max} distribution data at a distance on the order of $1.5(\delta x)^2/\lambda$ away from the peak. The value of λ has saturated (within error) upon application of these cuts and we estimate a best value of $\lambda = 72 \pm 9 \text{ g cm}^{-2}$.

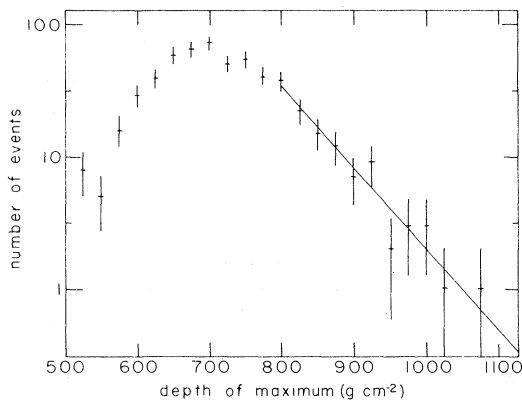


FIG. 5. Distribution of depth of maxima X_{max} for data whose fitting errors are estimated to be $\delta x < 125 \text{ g cm}^{-2}$. The slope of the exponential tail is $\lambda = 73 \pm 9 \text{ g cm}^{-2}$.

Note that protons are most likely the parents of the penetrating showers used in this analysis. According to the Monte Carlo simulations of Ellsworth *et al.*,⁵ no nuclei heavier than alphas could generate such penetrating showers. If alphas proved to be their parents they would have to dominate our entire data sample, an implication at variance with current composition measurements⁷ in this energy region which limit the mean atomic weight of cosmic-ray primaries to less than 1.8. Thus, the contamination of highly penetrating alphas in our data sample should be much less than 25%.

The above result for λ implies a value of $\lambda_n = 45 \pm 5 \text{ g cm}^{-2}$ or $\sigma_{p\text{-air}}^{\text{inel}} = 530 \pm 66 \text{ mb}$. The extraction of σ_{pp}^{tot} from $\sigma_{p\text{-air}}^{\text{inel}}$ is obviously model dependent. Using Glauber theory,⁸ a Gaussian profile distribution for the nucleus,⁹ and assuming that the nuclear slope parameter b is proportional to σ_{pp}^{tot} , as is the case for geometric scaling,¹⁰ we find

TABLE II. Best fits for the X_{max} absorption length λ as a function of data cuts $\delta x < \delta x_c$ on the errors in the depth of shower maximum. The data for $\delta x < 125 \text{ g cm}^{-2}$ are plotted in Fig. 5.

Error cut δx_c (g cm^{-2})	X_{max} absorption length λ (g cm^{-2})
175	74 ± 9
150	72 ± 10
125	73 ± 9
100	70 ± 12
75	75 ± 14
50	52 ± 27
best estimate	72 ± 9

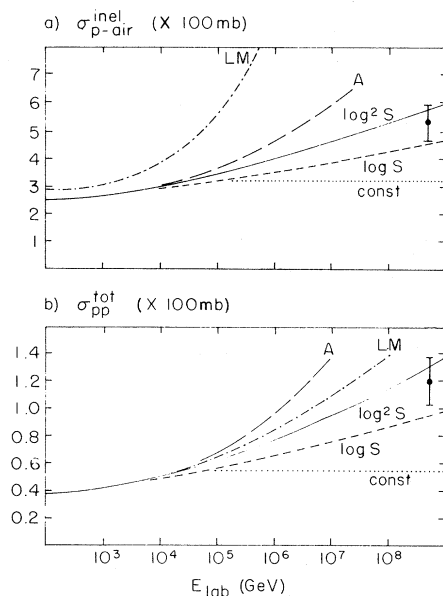


FIG. 6. Energy dependent (a) p -air inelastic and (b) pp total cross sections. The logs and $\log^2 s$ are extrapolations of fits up to energies of the CERN Intersecting Storage Rings. The curve labeled A is an extrapolation of the estimate of Afek *et al.* (Ref. 11) and LM stands for Leader and Maor (Ref. 12).

that $\sigma_{pp}^{\text{tot}} = 120 \pm 15 \text{ mb}$ at $s^{1/2} = 30 \text{ TeV}$. This value is plotted in Fig. 6 along with various extrapolations from lower energies. The model dependency in relating σ_{pp}^{tot} to $\sigma_{p\text{-air}}^{\text{inel}}$ is evident in the curves of Fig. 6 (note the curve labeled LM). In particular, if σ_{pp}^{tot} were to approach its black disk limit⁹ the value obtained here would represent a lower cross-sectional bound. We note that calculations of various nuclear inelastic cross sections using Glauber theory agree extremely well ($\pm 5\%$) with experimentally measured ones using a wide range of projectiles in the

energy range $20 \text{ GeV} < E < 1000 \text{ GeV}$.¹³ We also note that our results are consistent with those of Hara *et al.*¹⁴

We gratefully acknowledge partial support from the U.S. National Science Foundation for this research.

¹G. L. Cassiday *et al.*, in *Proceedings of the Workshop on Very High Energy Interactions, Philadelphia, 1982*, edited by M. Cherry, K. Lande, and R. I. Steinberg (Univ. of Pennsylvania Press, Philadelphia, 1982), pp. 72–82.

²G. L. Cassiday *et al.*, in *The Birth of the Universe, Proceedings of the Seventeenth Moriond Astrophysics Meeting, Les Arcs, France, 1982*, edited by J. Audouze and J. Tran Thanh Van (Editions Frontiers, Gif-sur-Yvette, France, 1982), pp. 331–346.

³R. Cady *et al.*, in *Proceedings of the Eighteenth International Cosmic Ray Conference, Bangalore, India, 1983*, edited by P. V. Ramana Murthy (Tata Institute of Fundamental Research, Bombay, 1983), EA 4-22.

⁴R. Cady *et al.*, in Ref. 3, OG 4-18.

⁵R. W. Ellsworth, T. K. Gaisser, T. Stanev, and G. B. Yodh, *Phys. Rev. D* **26**, 336 (1982).

⁶T. Gaisser and T. Stanev, in *Proceedings of the Workshop on Very High Energy Interactions, Philadelphia, 1982*, edited by M. Cherry, K. Lande, and R. I. Steinberg (Univ. of Pennsylvania Press, Philadelphia, 1982), pp. 125–135.

⁷J. Linsley, in Ref. 3.

⁸R. J. Glauber and G. Matthias, *Nucl. Phys.* **B21**, 135 (1970).

⁹V. Barger *et al.*, *Phys. Rev. Lett.* **33**, 1051 (1974).

¹⁰J. Dias de Deus, *Nucl. Phys.* **B59**, 231 (1974); A. J. Buras and J. Dias de Deus, *Nucl. Phys.* **B71**, 481 (1974).

¹¹Y. Afek *et al.*, *Phys. Rev. Lett.* **45**, 85 (1980).

¹²E. Leader and U. Maor, *Phys. Lett.* **43B**, 505 (1973).

¹³R. W. Ellsworth *et al.*, *Phys. Rev. D* **27**, 1183 (1983).

¹⁴T. Hara *et al.*, *Phys. Rev. Lett.* **50**, 2058 (1983).